

Chapter 6

Slopes of Multi-Element Isotope Plots of Fractionation in Photolysis of N₂O: A Mass-Dependent Theory for Isotopomers Where Two Effective Masses Contribute

[This chapter prepared for the *Journal of Chemical Physics*.]

Abstract

A single effective mass usually serves to determine the slope of a multielement isotope plot and to yield approximate agreement between the experimental data and a “mass-dependent” fractionation. The data typically treated are for reactions that involve with little change in total “bond order,” one bond broken and another formed. Instead, we treat a photolytic dissociation where the total bond order changes. In the present instance of the photolytic dissociation of N_2O , the computational and experimental results largely agree, but two effective masses are needed to understand intuitively the slopes of the multielement isotope plots, which range from 0.47 to 3.28. A linear combination of the main coordinates for the dissociation provides agreement with these numerical slopes. For the particular case of a multielement isotope plot of 448 vs 447 (which is also a usual three-isotope plot), the two-effective mass result reduces to the usual single mass case, so explaining why the slope value is ~ 0.5 in this case. The present theory also agrees with the experimental slopes in multielement isotope plots.

I. INTRODUCTION

Customarily, isotopic fractionation plots in the literature are those in which for some series of samples the isotopic enrichment of one isotope is plotted vs that of another, such as $^{17}\text{O}/^{16}\text{O}$ vs $^{18}\text{O}/^{16}\text{O}$.¹⁻³ The slope of the plot is then compared with theory, particularly the well-known Bigeleisen-Mayer theory.⁴ Other examples of such plots include those for the sulfur isotopes, and many others.^{5,6}

Recently, a related but different kind of fractionation plot has appeared in the literature, one in which the isotopic fractionation of one element is plotted versus that of another, e.g. Park et al.,⁷ Bindeman et al.,⁸ and Sturchio et al.⁹ In one of these multielement isotope plots, the enrichment in an N isotope was plotted versus that for an O isotope.⁷ In another case, the enrichment in S and O isotopes of volcanogenic sulfate aerosols was studied.⁸ In the other case, the Cl and O isotopic fractionation due to biodegradation of perchlorate was plotted.⁹ In the present paper, we explore multielement isotope fractionation plots and for concreteness focus on such a plot for a particular system, N_2O photolysis.

The photolysis of N_2O has been extensively studied in the literature, summarized in Part 1–3.¹⁰⁻¹² Prakash et al. also used a first-order expansion analysis to gain insight into the consequences of the theoretical expression for the slope of the oxygen three-isotope plot in photolytic fractionation of N_2O .¹³ The slope obtained by a first-order analysis for the oxygen mass-dependent effect agreed well with that obtained in detailed computations.

In the present article, a first-order analysis similar to that used for the previous result,¹³

but extended to other isotopomers is used. Previously 447 and 448 were measured relative to 446 and plotted as the usual three-isotope plot. Only the O isotope was varied. Now the N atoms are also varied yielding a “multielement” isotope fractionation plot. multielement isotope fractionation plots have appeared in the literature in Park et al.,⁷ Bindeman et al.,⁸, and Sturchio et al.⁹ The slopes of multielement isotope plots in the photolysis of N_2O vary from 0.47 to 3.28. We find that a simple single reduced mass no longer suffices to understand the theoretical results. All normal coordinates are now affected in the additional isotopomers in which the central N is varied. The experimental slopes in the multielement isotope plots are very close to the results obtained by the present first-order expansion analysis using reduced masses. To understand the detailed results of the numerical calculations of the slope of the multielement isotope plots for different isotopomers, we consider the physical nature of the photolysis coordinates of the photodissociation of N_2O and give an approximate theoretical expression of the mass effect in the multielement isotope fractionation plots.

II. THEORY

A. Absorption Cross Section

The theoretical procedure used to obtain absorption cross sections for the N_2O isotopomers was described previously,¹² and is briefly summarized here. UV photolysis of N_2O is essentially a direct dissociation, since the absorption spectrum is a broad envelope with a only weak structure superimposed. Thereby, the absorption cross section can be

obtained using the multidimensional reflection principle.^{14,15} The absorption cross section σ is given by¹¹

$$\begin{aligned}\sigma_{f\tilde{n}}(\omega) &= \frac{\pi\omega}{\hbar\epsilon_0c} \frac{1}{2\pi} \int_{-\infty}^{\infty} dt \langle \Psi_{\tilde{n}} | \vec{\mu}_{fi}^\dagger e^{-iH_f t/\hbar} \vec{\mu}_{fi} | \Psi_{\tilde{n}} \rangle e^{i(\omega+E_i/\hbar)t} \\ &\approx \frac{\pi\omega}{3\epsilon_0c} \int d\mathbf{Q} |\Psi_{\tilde{n}}(\mathbf{Q})|^2 |\vec{\mu}_{fi}(\mathbf{R})|^2 \delta(\hbar\omega - V_f(\mathbf{R}) + V_i(\mathbf{R}))\end{aligned}\quad (1)$$

where \mathbf{R} and \mathbf{Q} denote internal and normal coordinates, respectively. The transition dipole moment function $\vec{\mu}_{fi}(\mathbf{Q})$ is a transition between the ground and the excited electronic states i and f , respectively. The difference of potential energy surfaces between the electronic excited and ground states is denoted as $V_f(\mathbf{Q}) - V_i(\mathbf{Q})$. The probability density of the initial nuclear vibrational state \tilde{n} in the ground electronic state i is $|\Psi_{\tilde{n}}(\mathbf{Q})|^2 d\mathbf{Q}$.

B. Fractionation

Different isotopomers have the same potential energy function but differ in their normal mode frequencies and normal coordinates, and thereby differ in the width of the electronic ground state wave function, $\Psi_{\tilde{n}}(\mathbf{Q})$. Accordingly, they have different absorption cross sections at any wavelength, leading to a fractionation of the isotopomers by photodissociation, particularly in the wings of the absorption band. The photodissociation rate $J(\omega)$ of a molecule is given as

$$J(\omega) = \sigma_{total}(\omega) I(\omega) \phi(\omega), \quad (2)$$

where $I(\omega)$ is the photo flux at frequency ω and $\phi(\omega)$ is the quantum yield of the reaction at that ω . The quantum yield $\phi(\omega)$ is assumed to be unity in the photolysis of N_2O

due to the direct or nearly-direct nature of the photodissociation. The total absorption cross-section $\sigma_{total}(\omega)$ is obtained by adding the contributions at ω from all vibrational states in the electronic ground state, weighted by their thermal populations according to the Boltzmann distribution. The fractionation factor is dependent upon the ratio of the photolysis rates for the isotopomers A' and A and is written as

$$\epsilon_A^{A'} = \frac{J_{A'}(\omega)}{J_A(\omega)} - 1 = \frac{\sigma_{total}^{A'}(\omega)}{\sigma_{total}^A(\omega)} - 1. \quad (3)$$

In a multielement isotope plot the ϵ value of one isotopomer is plotted versus that of another, both relative to the same isotopomer.

C. A First Order Analysis of Mass Dependence

In the present paper, we extend the first-order expansion for the slope of the oxygen three-isotope plot¹³ to a more general case. $\vec{\mu}_{f_i}(\mathbf{R})$ and $V_f(\mathbf{R})$ in equation (1) are independent of isotopic substitutions since \mathbf{R} is mass independent. We recall that $|\Psi_n(\mathbf{Q})|^2 d\mathbf{Q}$ is mass dependent because the \mathbf{Q} are the normal coordinates of a isotopomer and they are mass dependent. A Taylor series expansion of the total absorption cross section, σ_{total} , is used to the first order. If the reduced mass μ_i of the coordinate x_i in the \mathbf{X} coordinate space is changed due to isotopic substitution, the first order expansion treatment for the entire expression of the cross section involves the first order difference in reciprocal masses $\Delta(\mu_i) = \mu_i^{A'} - \mu_i^A$ for the two isotopomers, A and A' :

$$\sigma_{total}^{A'}(\omega) \approx \sigma_{total}^A(\omega) + \sum_i \frac{\partial \sigma_{total}^A(\omega)}{\partial \mu_i} \Delta(\mu_i). \quad (4)$$

According to the physical properties of photodissociation of N_2O , in which the N_2 bond length changes only slightly as a result of the photolysis, there are two different reduced masses crucial in the fractionation. Since the photoabsorption is promoted by the bending modes and since the asymmetric stretching mode of N_2O leads to the photolysis products N_2 and O , both motions are important in the dissociation. They can be described in terms of two reduced masses, one being that of the oxygen atom and the nitrogen molecule, and the second being the oxygen atom and the nitrogen atom to which it is bonded, since the NN bond length is not very different in N_2O and N_2 . The μ_k that is the best choice to represent this photodissociation is some linear combination of the two reduced masses of the above two coordinates for a molecule labeled as $\text{N}^1\text{N}^2\text{O}$, $1/\mu_1 = 1/(m_{\text{N}^1} + m_{\text{N}^2}) + 1/m_{\text{O}}$ and $1/\mu_2 = 1/m_{\text{N}^2} + 1/m_{\text{O}}$.

With this assumption that some linear combination of the μ_i s in equation (4), denoted by μ_k , the absorption cross section becomes

$$\sigma_{total}^{A'}(\omega) \approx \sigma_{total}^A(\omega) + \frac{\partial \sigma_{total}^A(\omega)}{\partial \mu_k} \Delta(\mu_k). \quad (5)$$

Thus, the slope β of the $\epsilon_A^{A''}$ vs $\epsilon_A^{A'}$ plot based on the above first-order expansion is obtained as

$$\beta = \frac{\mu_k^{A''} - \mu_k^A}{\mu_k^{A'} - \mu_k^A}, \quad (6)$$

where A usually is the isotopomer with the most abundant isotopes, the A' and A'' isotopomers have isotope substitution on the same element. If there are substitutions on different elements, an experience factor f_{O}^{N} should be included since the linear combination of μ_1 and μ_2 would overemphasize the contribution from oxygen. The more general form

of equation (6) is

$$\beta = f_{\text{O}}^{\text{N}} \frac{\mu_k^{A''} - \mu_k^A}{\mu_k^{A'} - \mu_k^A}, \quad (7)$$

where the A' and A'' isotopomers have isotope substitution at oxygen and nitrogen, respectively, and the current fitted f_{O}^{N} value is 5.2 in the N_2O photolysis. And so the ratio of the relative difference of the reduced masses μ_k s of isotopomers in equations (6) and (7) appears as a slope in each multielement isotope plot.

III. RESULTS AND DISCUSSION

A. Slopes of multielement Isotope Plots of Fractionation

The purpose of the present article is to understand the slopes for the different comparisons of isotopomers, given by the detailed computations in Chen et al.¹² To the extent the approximate perturbation model described earlier is used.¹³ The calculated slopes of a multielement isotope plots for various isotopomers are given in Table I, where the subscript 446 is omitted, the fractionation obtained by the ratio of the absorption cross-section relative to that for this most abundant isotopomer of N_2O . They are compared there with the detailed computational results of Chen et al.¹²

We use weighting factors, 91% and 9%, respectively, to obtain best agreement with the results of the numerical calculations, $\mu_k = 0.91\mu_1 + 0.09\mu_2$. Presumably the derivation of μ_1 here is because the process is mainly a dissociation into $\text{N}_2 + \text{O}$, while the μ_2 reflects a torque acting on the N^2 due to the large bending angle of the excited N_2O , as well as in part the N_2 -O repulsion. The approximate slopes obtained using μ_k and equations (6)

TABLE I: Calculated slopes of multielement isotope plots. The Pearson's coefficient of the linear regression of the theoretical calculations are better than 0.99.

	Lin. Comb. Approx.	233 K ^a	283 K ^a	298 K ^a
Isotope Substitution at a Single Element				
ϵ^{448} vs ϵ^{447}	0.512	0.537	0.538	0.539
ϵ^{456} vs ϵ^{546}	0.826	0.820	0.829	0.844
ϵ^{556} vs ϵ^{456}	0.559	0.568	0.570	0.572
ϵ^{556} vs ϵ^{546}	0.461	0.471	0.474	0.481
Isotope Substitution at Both Elements				
ϵ^{448} vs ϵ^{456}	0.993	1.003	0.999	1.003
ϵ^{448} vs ϵ^{546}	0.820	0.850	0.833	0.828
ϵ^{448} vs ϵ^{556}	1.777	1.766	1.756	1.756
ϵ^{447} vs ϵ^{456}	1.937	1.861	1.859	1.867
ϵ^{447} vs ϵ^{546}	1.600	1.577	1.549	1.540
ϵ^{447} vs ϵ^{556}	3.468	3.278	3.267	3.269

^a The slope is obtained by fitting the result of numerical theory in reference 12.

and (7) are seen in Table I to be very close to the linear fit of the detailed computational results. They are also seen to be very different from the usual 0.5 slope for a fractionation of an isotope with a mass unit difference compared with that for an isotope with two mass units difference.

The use of two coordinates and their combination to describe the mass dependence in a reaction appears to be novel although multielement isotope fractionation plots are given in the literature, such as Park et al.,⁷ Bindeman et al.,⁸, and Sturchio et al.⁹ This case of two effective masses is also closely related to a related reaction coordinate introduced by Klippenstein in variational RRKM to find the transition state of a thermal barrierless unimolecular dissociation reaction.¹⁶ The best reaction coordinate to describe the system was neither the length of the breaking bond (here N²-O) nor the distance between the center of masses of the dissociation fragments (here, that of N¹-N² and O), but rather a linear combination of these two coordinates. The interpretation of the present results for a dissociation invoking two coordinates and two effective masses may also apply to multielement isotope plots for other direct photodissociations, but at this stage of their interpretation would need to be examined on a case by case basis.

In the formation of N₂ and O from N₂O, both bending and asymmetric stretching modes are directly involved in the reaction coordinate of photodissociation. The slopes obtained by μ_k and by the reduced mass of each normal coordinate are compared in Table II with the full theoretical results. Since the symmetric stretching mode has little correlation with the dissociation reaction, its slopes gives strange values in all nitrogen isotopomers (see Table II).

TABLE II: Slopes of multielement isotope plots in isotopic nitrogen substituted istopomers. The slopes obtained by linear combination method of reduced mass (μ_k) and normal coordinates are compared with the full theoretical results.

Method	ϵ^{448} vs ϵ^{447}	ϵ^{556} vs ϵ^{456}	ϵ^{556} vs ϵ^{546}	ϵ^{456} vs ϵ^{546}
Numerical Theory ^a	0.537	0.572	0.471	0.820
Lin. Comb. Approx. (μ_k)	0.512	0.559	0.461	0.826
Asymmetric Stretching	0.535	0.794	0.186	0.234
Symmetric Stretching	0.510	-0.033	1.042	-31.240
Bending	0.527	0.782	0.199	0.254

^a The temperature is 233 K.

B. Comparison with Experiments

A multielement isotope plots calculated by Chen et al.,¹² are shown in Fig. 1 for ϵ^{448} vs ϵ^{447} , in Fig. 2 for ϵ^{556} vs ϵ^{456} , in Fig. 3 for ϵ^{556} vs ϵ^{546} , and in Fig. 4 for ϵ^{456} vs ϵ^{546} . All computational results show reasonable agreement with available experimental data in laboratories.^{17,18} They also give good agreement with the slopes of multielement isotope plots calculated by a first-order approximation with the linear combine coordinate, as given in Table I.

However, the observations of the slopes of ϵ^{456} vs ϵ^{546} , ϵ^{448} vs ϵ^{456} , and ϵ^{448} vs ϵ^{546} in the stratosphere are listed in Table III.^{7,19,20} The slopes of ϵ^{456} vs ϵ^{546} , and ϵ^{448} vs ϵ^{546} obtained by our linear combination approximation are within the values of some experimental error. However, the linear combination approximation gives a significantly smaller value in ϵ^{448} vs ϵ^{456} . This difference may be due to the anomalous mass effect of N_2O caused by other chemical reactions in troposphere and lower stratosphere, as discussed by McLinden et al. using a global model.²¹

C. Applied to Other Systems

The first-order expansion method with a linear combination of two effective reduced masses give a successful approximation in the slopes of the multielement isotope plots in the N_2O photolysis. This method may be extended to other mass-dependent reactions once the rate is dominated by a single rate-controlling step. For example, a multielement isotope plot of oxygen and chlorite isotopic fractionation is obtained by studying

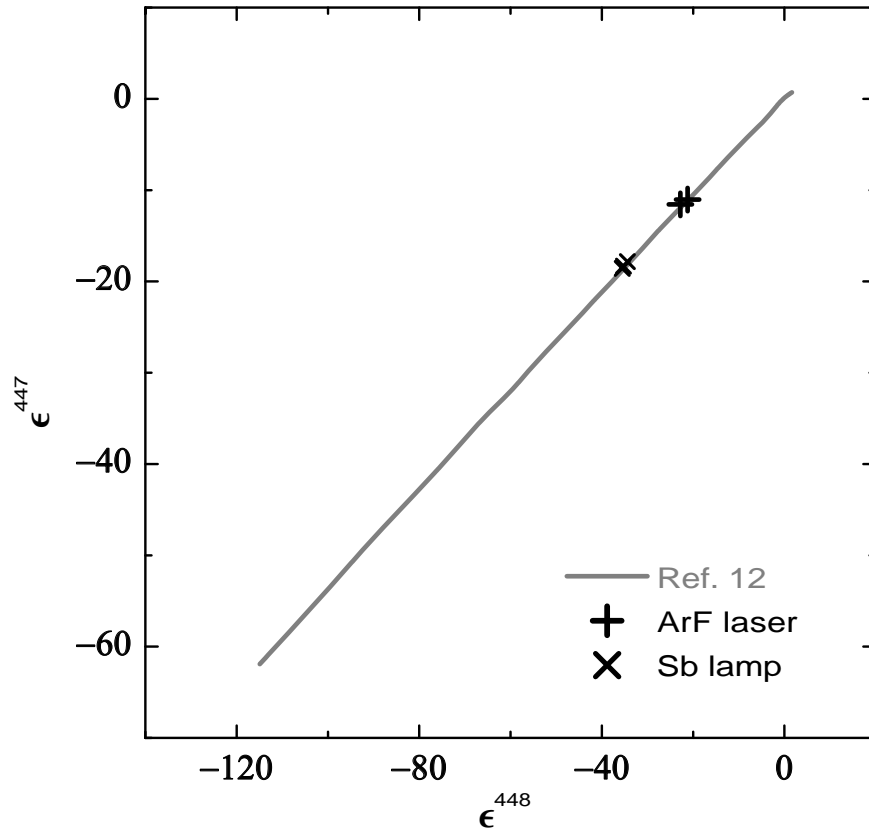


FIG. 1: Three-isotope plot of oxygen isotopologues of N_2O in units of per mil. The experimental data are from Röckmann et al.¹⁷ The linear regression slope of the numerical theory at 233 K obtained by Chen et al.¹² is 0.537.

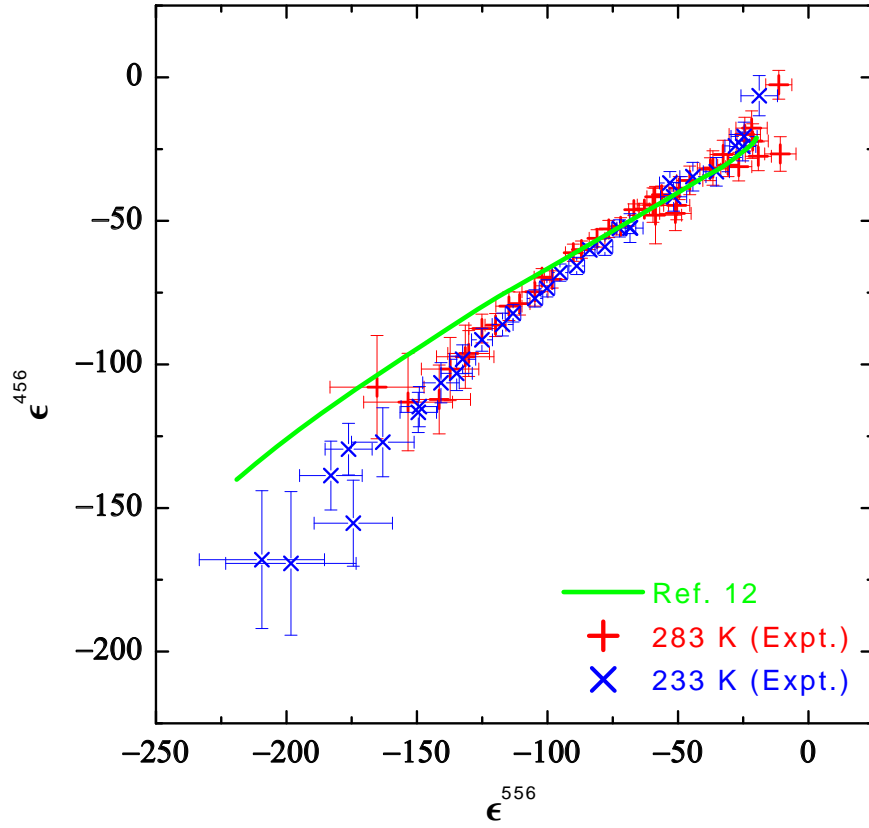


FIG. 2: multielement isotope plot of ϵ^{556} vs ϵ^{456} in units of per mil. The experimental data are from von Hessberg et al.¹⁸ The linear regression slope of the numerical theory at 233 K obtained by Chen et al.¹² is 0.572.

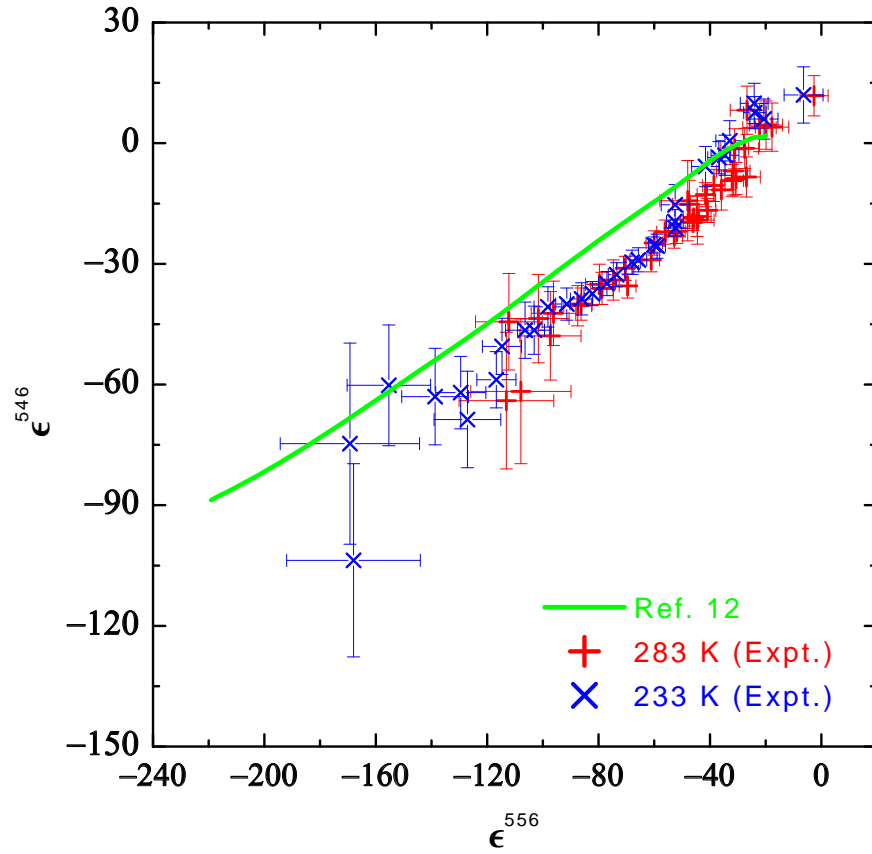


FIG. 3: multielement isotope plot of ϵ^{556} vs ϵ^{546} in units of per mil. The experimental data are from von Hessberg et al.¹⁸ The linear regression slope of the numerical theory at 233 K obtained by Chen et al.¹² is 0.471.

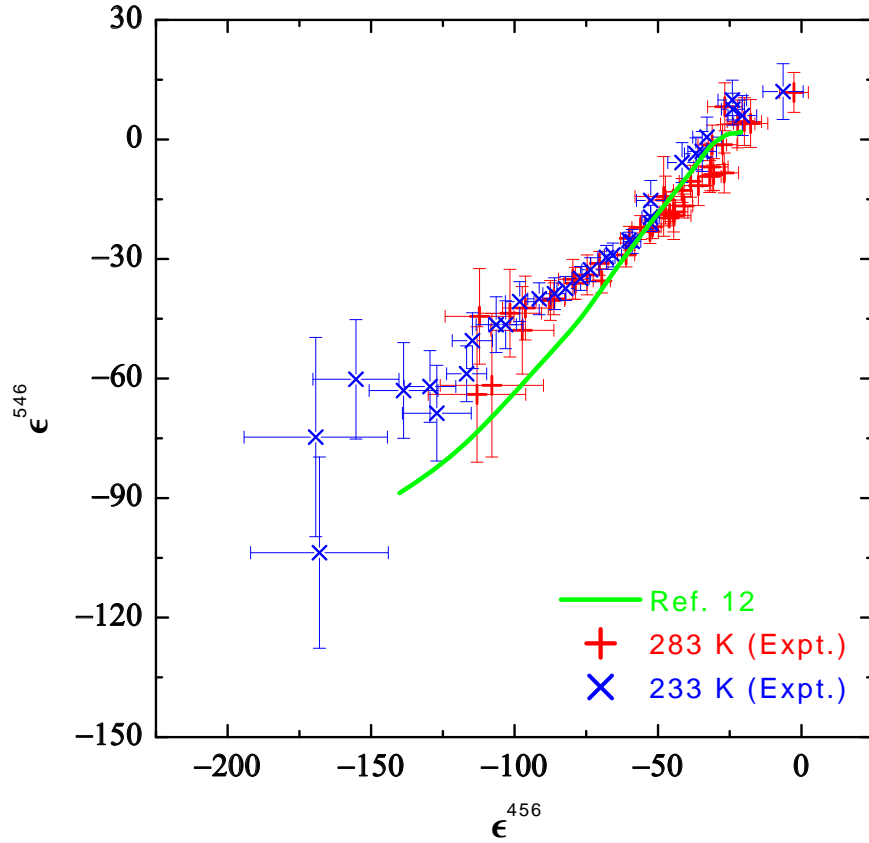


FIG. 4: multielement isotope plot of ϵ^{456} vs ϵ^{546} in units of per mil. The experimental data are from von Hessberg et al.¹⁸ The linear regression slope of the numerical theory at 233 K obtained by Chen et al.¹² is 0.820.

TABLE III: The slopes of multielement isotope plots. The number given in parentheses are the values of 2σ uncertainties in experiments.

	ϵ^{456} vs ϵ^{546}	ϵ^{448} vs ϵ^{456}	ϵ^{448} vs ϵ^{546}
Lin. Comb. Approx.	0.826	0.993	0.820
	Park et al. ⁷		
Photolysis	0.42 (± 0.03)	1.55 (± 0.06)	0.65 (± 0.04)
< 200 ppbv SOLVE ^a	0.38 (± 0.07)	1.70 (± 0.07)	0.64 (± 0.12)
< 200 ppbv POLARISII ^b	0.56 (± 0.27)	1.58 (± 0.21)	0.82 (± 0.29)
< 200 ppbv All	0.43 (± 0.06)	1.65 (± 0.06)	0.68 (± 0.20)
> 200 ppbv All	0.38 (± 0.14)	1.70 (± 0.17)	0.53 (± 0.22)
	Toyoda et al. ^{20 c}		
> 24.1 km	0.38 (± 0.03)	1.66 (± 0.13)	0.63 (± 0.04)
< 24.1 km	0.38 (± 0.13)	1.99 (± 0.66)	0.77 (± 0.34)
	Röckmann et al. ^{19 c}		
All	0.50 (± 0.03)	1.54 (± 0.07)	0.76 (± 0.04)
> 200 ppbv	0.61 (± 0.12)	1.51 (± 0.24)	0.92 (± 0.22)

^a Stratospheric aerosol and gas experiment III Ozone Loss and Validation Experiment

(SOLVE).²³

^b Photochemistry of Ozone Loss in the Arctic Region in Summer (POLARIS) mission from

April and September 1997.²⁴

^c The slopes shown here for the Toyoda et al.²⁰ and Röckmann et al.¹⁹ data were calculated by

Park et al.⁷ from their original publications.

the biodegradation of perchlorate.⁹ The widely accepted pathway now of biological degradation have been reported as follows: (i) perchlorate (ClO_4^-) is first reduced to chlorate (ClO_3^-) and then to chlorite (ClO_2^-) by the perchlorate reductase, and (ii) the ClO_2^- then undergoes a disproportionation reaction catalyzed by the chlorite dismutase to yield Cl^- and O_2 .²² However, the detailed mechanism at the molecular level is still absent. If the rate-controlling step is the $\text{E}_1 \cdot \text{O}_x \text{Cl} - \text{O} \cdot \text{E}_2 \rightarrow \text{E}_1 \cdot \text{O}_x \text{Cl} + \text{O} \cdot \text{E}_2$ reaction (where E_1 and E_2 are the crucial parts of the enzyme binding with ClO_{x+1} and the charge state is omitted in the reaction equation), two effective reduced mass to describe the mass-dependent properties of the reaction may be $1/\mu_1 = 1/m_{\text{Cl}} + 1/m_{\text{O}}$ and $1/\mu_2 = 1/m_{\text{E}_1 \cdot \text{O}_x \text{Cl}} + 1/m_{\text{O} \cdot \text{E}_2}$. The coefficient for the linear combination of μ_1 and μ_2 can be determined by the fractionation experiments of oxygen or chlorine isotopic substitutions. The slope in the corresponding multielement isotope plot may be estimated by using equation (7).

The observed enrichments in S and O isotopes of volcanogenic sulfate aerosols on the multielement isotope plot by Bindeman et al.⁸ are scattered too much to define a slope. It may involves many independent reactions, which would make it very difficult to apply the current method.

IV. CONCLUSIONS

Using a first-order expansion method with a newly defined photolysis reduced mass and coordinate obtained by a linear combination, the slopes of the multielement isotope plots are close to the theoretical detailed calculation of photodissociation fractionation of N_2O , and are similar to experimental results. The concept of photolysis coordinate defined by a

linear combination of coordinates is a fruitful one in the present case and can be extended to study the mass-dependent effect of other direct or nearly direct photodissociation reactions or of other chemical reaction with a single rate-controlling step.

Acknowledgments

It is a pleasure to acknowledge the support of this research by the National Science Foundation.

- ¹ R. N. Clayton, L. Grossman, and T. K. Mayeda, *Science* **182**, 485 (1973).
- ² M. H. Thiemens, *Science* **283** (1999).
- ³ M. H. Thiemens, *Annu. Rev. Earth Planet. Sci.* **34** (2006).
- ⁴ J. Bigeleisen and M. G. Mayer, *J. Chem. Phys.* **15**, 261 (1947).
- ⁵ R. E. Criss and J. Farquhar, *Rev. Mineral. Geochem.* **68** (2008).
- ⁶ S. Amari, L. R. Nittler, E. Zinner, K. Lodders, and R. S. Lewis, *Astrophys. J.* **559** (2001).
- ⁷ S. Y. Park, E. L. Atlas, and K. A. Boering, *J. Geophys. Res. - Atmos.* **109**, D01305 (2004).
- ⁸ I. N. Bindeman, J. M. Eiler, B. A. Wing, and F. J., *Geochimica et Cosmochimica Acta* **71**, 2326 (2007).
- ⁹ N. C. Sturchio, J. K. Böhlke, A. D. Beloso, Jr., L. J. Heraty, and P. B. Hatzinger, *Environ. Sci. Technol.* **41**, 2796 (2007).
- ¹⁰ M. K. Prakash, J. D. Weibel, and R. A. Marcus, *J. Geophys. Res.-Atmos.* **110**, D21315 (2005).
- ¹¹ W. C. Chen, M. K. Prakash, and R. A. Marcus, *J. Geophys. Res.-Atmos.* **113**, D05309 (2008).
- ¹² W. C. Chen, R. A. Marcus, and S. Nanbu, **manuscript** (2009).
- ¹³ M. K. Prakash and R. A. Marcus, *J. Chem. Phys.* **123**, 174308 (2005).
- ¹⁴ E. J. Heller, *J. Chem. Phys.* **68**, 2066 (1978).
- ¹⁵ R. Schinke, *Photodissociation Dynamics* (New York: Cambridge University Press, 1993).
- ¹⁶ S. J. Klippenstein, *Chem. Phys. Lett.* **214**, 418 (1993).

- ¹⁷ T. Röckmann, J. Kaiser, J. N. Crowley, C. A. M. Brenninkmeijer, and P. J. Crutzen, *Geophys. Res. Lett.* **28**, 503 (2001).
- ¹⁸ P. von Hessberg, J. Kaiser, M. B. Enghoff, C. A. McLinden, S. L. Sorensen, T. Röckmann, and M. S. Johnson, *Atmos. Chem. Phys.* **4**, 1237 (2004).
- ¹⁹ T. Röckmann, J. Kaiser, C. A. M. Brenninkmeijer, J. N. Crowley, R. Borchers, W. A. Brand, and P. J. Crutzen, *J. Geophys. Res. - Atmos.* **106**, 10403 (2001).
- ²⁰ S. Toyoda, N. Yoshida, T. Urabe, S. Aoki, T. Nakazawa, S. Sugawara, and H. Honda, *J. Geophys. Res.-Atmos.* **106**, 7515 (2001).
- ²¹ C. A. McLinden, M. J. Prather, and M. S. Johnson, *J. Geophys. Res.-Atmos.* **108** (2003).
- ²² J. D. Coates and L. A. Achenbach, *Nature Rev. Microbiol.* **2** (2004).
- ²³ P. A. Newman, N. R. P. Harris, A. Adriani, G. T. Amanatidis, J. G. Anderson, G. O. Braathen, W. H. Brune, K. S. Carslaw, M. S. Craig, P. L. DeCola, et al., *J. Geophys. Res.-Atmos.* **107** (2002).
- ²⁴ P. A. Newman, D. W. Fahey, W. H. Brune, and M. Kurylo, *J. Geophys. Res.-Atmos.* **104**, 26481 (1999).